Nitriding of iron boride to hexagonal boron nitride

T. E. WARNER, D. J. FRAY
Department of Materials Science and Metallurgy, University of Cambridge, Pembroke Street, Cambridge CB2 3QZ, UK
E-mail: djf25@cam.ac.uk

A process for preparing hexagonal boron nitride (h-BN) from iron boride (FeB) has been described for the first time. FeB powder was nitrided in ammonia at 700 K for 24 hours yielding non-crystalline BN and ζ-Fe_2N. Subsequent annealing in ammonia for 1 hour at 1273 K resulted in a mixture of crystalline h-BN together with α-Fe, ε-Fe_3N and γ'-Fe_4N. The morphology of the product grains is described. This comprises an iron nitride core loosely encapsulated in a foliated BN layer. The open nature of the product layer may account for the relatively low temperature (700 K) required for the nitriding reaction. These iron containing phases were removed with dilute mineral acid leaving h-BN and trace amounts of FeB_{49}. © *2000 Kluwer Academic Publishers*

1. Introduction

This work is part of a programme of investigating the feasibility of upgrading relatively inexpensive ferroalloys to valuable materials. This can involve simply the separation of the valuable element in the ferroalloy from the iron component, as in the recent example of nitriding ferrochrome to chromium metal via a chromium nitride intermediate [1]. Alternatively, it can involve the production of a valuable compound containing the principle element from the ferroalloy. Here, the latter approach has been explored for the preparation of hexagonal boron nitride (h-BN) from ferroboron (FeB). FeB is currently produced on an industrial scale in the steel industry. Conventional processes for the commercial production of h-BN involve the nitriding (with ammonia or urea) of either boric acid (H_3BO_3) or borax anhydride ($Na_2B_4O_7$). These are reported to be long and complex processes resulting in calcium, sodium and phosphorus contamination within the product [2].

In 1951 Kiessling and Liu described the thermal stability of several metal borides including the iron borides Fe_2B and FeB in streaming ammonia [3]. They concluded that Fe_2B was slightly less kinetically stable than FeB and attributed this to the difference in reactivity of the isolated (interstitial) boron atoms in Fe_2B compared with the B-B atomic chains in FeB towards ammonia. The products comprised boron nitride and various proportions of the iron nitrides (ζ-Fe_2N, ε-Fe_3N and γ'-Fe_4N) together with α-Fe depending upon the temperature of reaction. At 673 K (the lowest temperature reported for observable reaction) FeB underwent an incomplete reaction yielding ζ-Fe_2N and the unconfirmed presence of BN.

The work presented here develops from these earlier observations. A kinetic and mechanistic study was undertaken to find the optimal conditions for converting FeB to h-BN. Ammonia has kinetic and thermodynamic advantages over nitrogen gas as the nitriding reagent for metals and alloys. Hägg noted in 1930 that the high reactivity of the resulting atomic nitrogen when using ammonia resulted in metal nitrides forming at lower temperatures [4]. This can be attributed to the substantially lower mean bond enthalpy for the N-H bond in ammonia (388 kJ mol^{-1}) [5] than the N≡N triple bond in nitrogen gas (946 kJ mol^{-1}) [5]. Furthermore, there is a huge release in free energy associated with the dissolution of ammonia (especially at elevated temperature) on account of the large increase in entropy for the dissociation reaction:

$$2NH_3(g) \rightarrow N_2(g) + 3H_2(g).$$
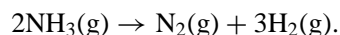
2. Experimental procedure

Ferroboron powder (18.89 wt.% boron) was supplied from London & Scandinavian Metallurgical Company Ltd. and was analysed by powder X-ray diffractometry and shown to correspond to the phase FeB (ICDD card: 32-463). In typical experiments, 1.200 g aliquots of FeB powder (-45 μm) were placed evenly in recrystallised alumina crucibles ($25 \times 100 \times 15$ mm) and positioned at the centre of the working tube ($40 \times 50 \times 1000$ mm) of a Lenton 1600 furnace. The working tube was sealed at both ends with silicon rubber stoppers, through which stainless-steel tubes were inserted to provide a gas inlet and outlet at opposite ends of the tube. The inlet gas flow rate was controlled and monitored with a suitable flow meter (CT Platon Ltd), whilst the outlet gas passed through two Drechsel washbottles. Bottled ammonia gas (Technical grade) was supplied by Air Products Ltd. The temperature was measured with a R-type thermocouple positioned close to the sample within the working tube.

Prior to furnace heating, the working tube was flushed with argon (100 ml/minute) for 1 hour. The furnace was then heated at a rate of 5°C/minute and

held at a predetermined temperature for 24 hours. After cooling to room temperature (5°C/minute) the furnace working tube was flushed with argon before opening. The product was removed, weighed, then analysed by powder X-ray diffractometry using a Philips diffractometer PW1710 with Cu K_{α_1} radiation ($\lambda = 1.54050$ Å). The peak positions in the powder pattern were compared with data in the ICDD files for phase identity. Samples of the product material were set into blocks of room temperature setting epoxy resin then ground and polished in preparation for SEM and optical microscopy studies. Observations of the product grains in cross-section were made using a Joel JSM-5800LV scanning electron microscope (with an EDXA attachment) and a Zeiss Axitech 25HC optical microscope (with camera attachment).

3. Results and discussion

The percentage increase in mass accompanying the nitriding of FeB in flowing ammonia at various temperatures is shown in Fig. 2. The optimum peak in mass gain (≈ 32 wt. %) occurs at approximately 700 K and corresponds to almost full nitriding as depicted by the following metastable reaction (see Fig. 1):

$$2FeB + 3NH_3(g) \rightarrow 2BN + Fe_2N + 4.5H_2(g).$$

This tallies with the ζ-Fe$_2$N phase identified in the XRD powder pattern for the product material (see Fig. 3). The very broad peaks for the ζ-Fe$_2$N phase suggests that a mixture of non-stoichiometric compositions are present here. Since iron nitrides are assumed to be metastable phases within the Fe-N binary system at atmospheric pressure [7], the occurrence of ζ-Fe$_2$N implies a state of non-equilibrium during the nitriding process due to the large over-pressure created by the decomposition of ammonia. The absence of any characteristic peaks in the powder pattern for crystalline boron nitride together with a very broad band at $2\theta \approx 20$–$30°$ suggests that the boron nitride is amorphous. Amorphous and sev-
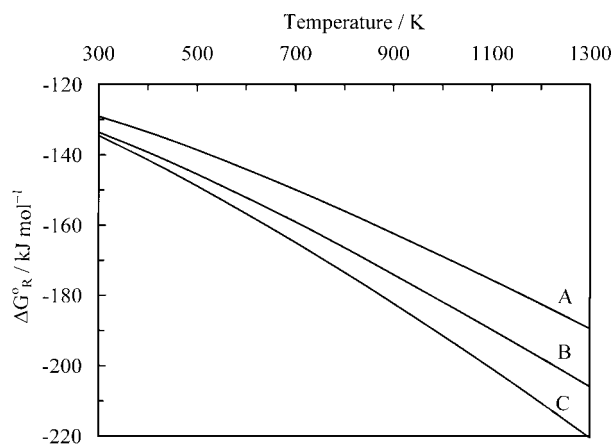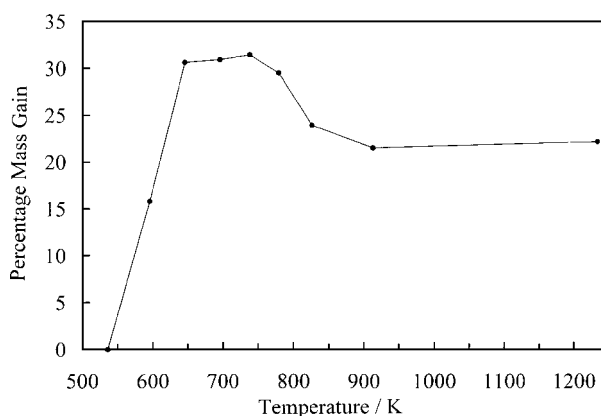
Figure 2 Plot of percentage mass gain as a function of reaction temperature for the nitriding of 0.200 g FeB in flowing ammonia gas after 24 hours.
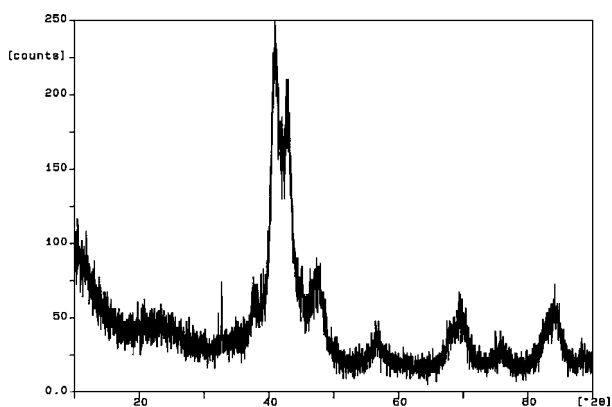
Figure 3 XRD powder pattern of the product material after nitriding at 645 K for 24 hours revealing broad peaks for ζ-Fe$_2$N (ICDD card: 6-656).

eral crystallographically disordered structures for BN are known in the literature and their existence is essentially due to the nature of the stacking sequence of the a-b planes in the layered material along the c-axis [8].

Fig. 4 shows a cross-section of the product grains under reflected light microscopy. The highly reflective core corresponds to ζ-Fe$_2$N whilst the less reflective material corresponds to BN. The exfoliated petal-like morphology of the BN periphery would account for the favourable reaction rates even at this moderate temperature (700 K). It suggests there is an outward diffusion of boron atoms from the core of the ferroboron grains whilst the fragmented nature of this product layer would cause little obstruction to the inward gaseous diffusion of ammonia to the reaction interface.

Fig. 5 shows the XRD powder pattern of the product material after nitriding at the higher temperature of 1073 K for 24 hours. The formation of the nitrogen deficient phases ε-Fe$_3$N and γ'-Fe$_4$N tallies with the lower mass gain (23%). The dominant peak for hexagonal boron nitride is just detectable at $2\theta \approx 26.7°$ (cf. ICDD card: 45-1171, viz. $2\theta = 26.7164°$), indicating that structural ordering is taking place by this temperature. A scanning electron microscope back scattered image for one of these grains in cross section is shown in Fig. 6. The exfoliated BN layer is again clearly evident.
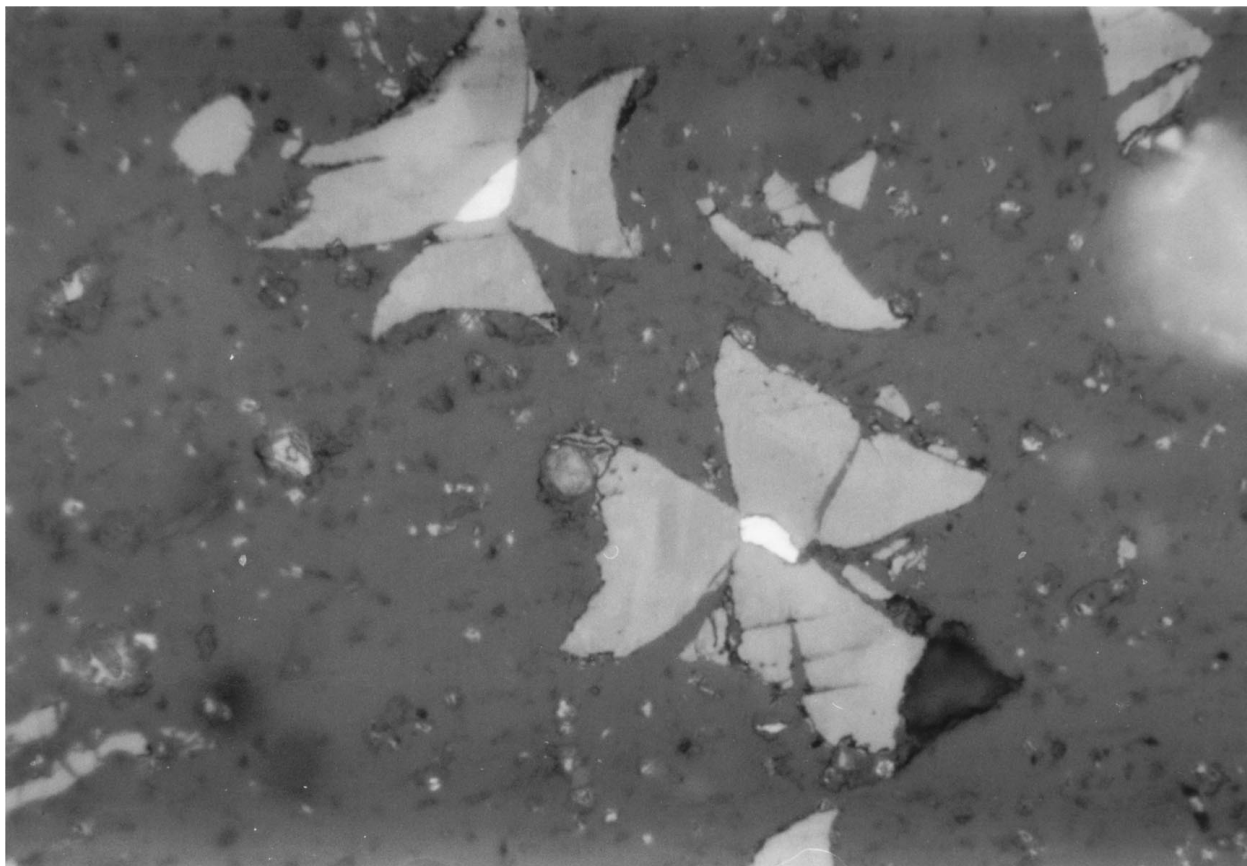
Figure 1 Plots of Gibbs functions for the following nitriding reactions: A: $2FeB + 3NH_3(g) \rightarrow 2BN + Fe_2N + 4.5H_2(g)$; B: $2FeB + 3NH_3(g) \rightarrow 2BN + 0.5Fe_4N + 4.5H_2(g) + 0.25N_2(g)$; C: $2FeB + 3NH_3(g) \rightarrow 2BN + 2Fe + 4.5H_2(g) + 0.5N_2(g)$; Thermodynamic data adopted from reference [6].

Figure 4 Reflected-light microscope image of a polished cross-section of product grains after nitriding at 645 K for 24 hours. Image reveals a reflective iron nitride core with an exfoliated boron nitride rim exhibiting a "petal-like" morphology. Image: $100 \times 144\ \mu$m.
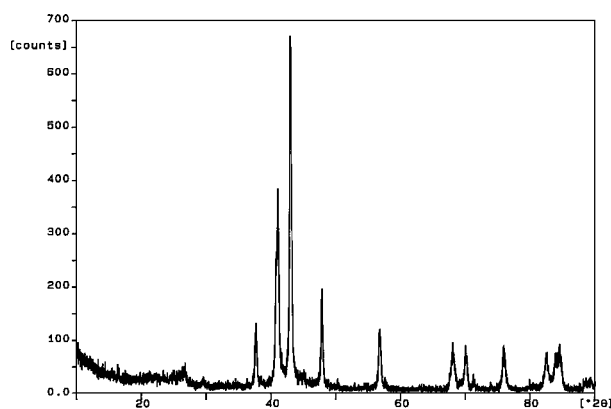

Figure 5 XRD powder pattern of the product material after nitriding at 1073 K for 24 hours revealing peaks for ε-Fe$_3$N and γ'-Fe$_4$N (ICDD cards: 1-1236 and 6-627).

The lower back scattering intensity for BN reflects the low atomic masses of boron and nitrogen. The iron rich core (ε-Fe$_3$N) is apparent from the accompanying EDXA iron map shown in Fig. 7.

Fig. 8 shows the XRD powder pattern for material that has been reacted with ammonia at 673 K for 24 hours then followed by an *in-situ* annealing period in flowing ammonia of 1 hour at 1273 K in an attempt to fully crystallise the BN. The major peak for h-BN is clearly evident at $2\theta \approx 26.7°$. The material is accompanied by the nitrogen deficient metastable assemblage: α-Fe, ε-Fe$_3$N and γ'-Fe$_4$N.

This product material was washed with warm 1 M hydrochloric acid solution then filtered through a Buchner funnel with an attached sintered glass filter. The grey solid residue was dried in air and observed under a reflected light microscope. The material comprised predominantly colourless grains interspersed with a few glistening black grains. The XRD powder pattern for this material is shown in Fig. 9. All the diffraction peaks are accountable for. The major phase corresponds to h-BN (ICDD card: 45-1171), whilst the few remaining minor peaks correspond to trace amounts of FeB$_{49}$ (ICDD card: 39-418). The acid solution has effectively removed the iron and iron nitrides from the product. The glistening black grains are therefore assumed to be FeB$_{49}$. The FeB$_{49}$ is likely to be an impurity accompanying the FeB in the ferroboron starting alloy and would account for the excess boron content of the alloy (18.89 wt. %) vis à vis (16.22 wt. %) in stoichiometric FeB.

4. Conclusions

Boron nitride with a non-crystallised structure has been prepared by reacting iron boride (FeB) with ammonia. Complete nitriding of the boron content (within a period of 24 h) was achieved at temperatures >650 K, in which the BN product was accompanied with ζ-Fe$_2$N. At reaction temperatures >900 K, BN was accompanied with the nitrogen deficient phases ε-Fe$_3$N and γ'-Fe$_4$N. Some structural ordering within the BN was detected at 1073 K and, by 1273 K it had crystallised as hexagonal BN.
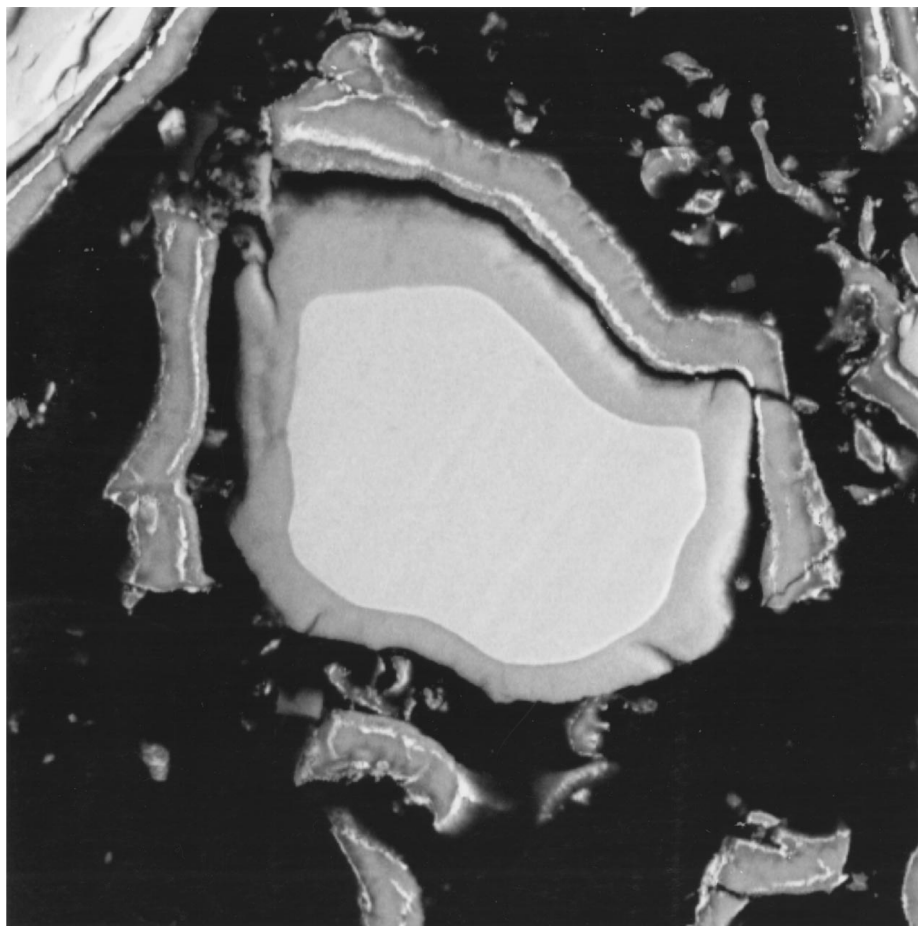
Figure 6 SEM back scattered image of a polished cross-section of one of the product grains after nitriding at 1073 K for 24 hours. Image reveals the iron nitride core with an exfoliated boron nitride rim. Image: 100×100 μm.
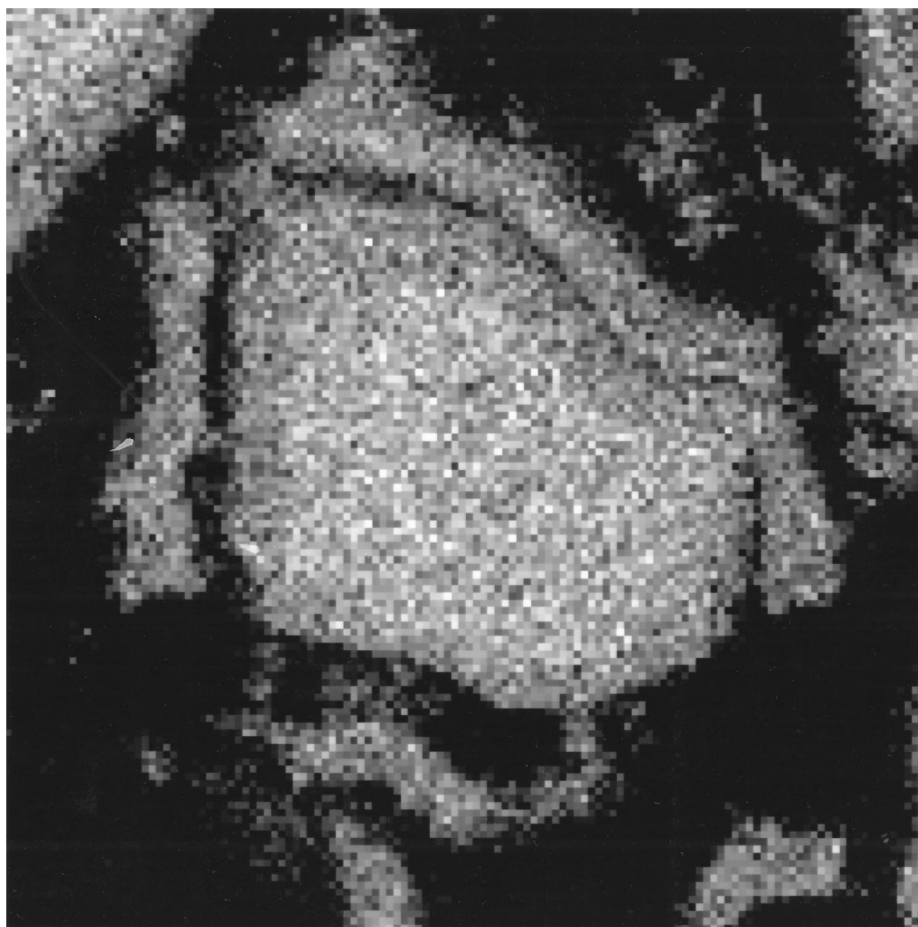

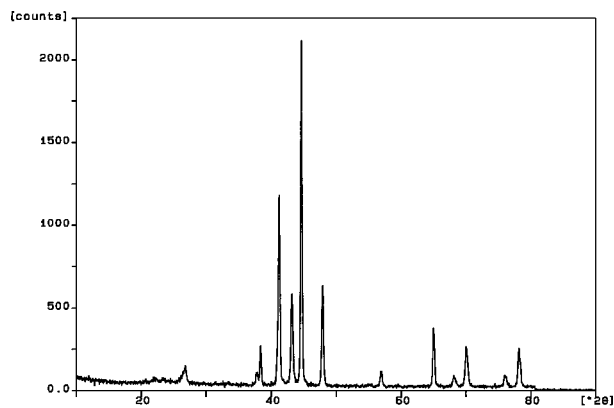*Figure 7* EDXA iron map of image in Fig. 6.

Figure 8 XRD powder pattern of the product material after nitriding at 773 K for 24 hours followed by an *in-situ* annealing period of 1 hour at 1273 K.
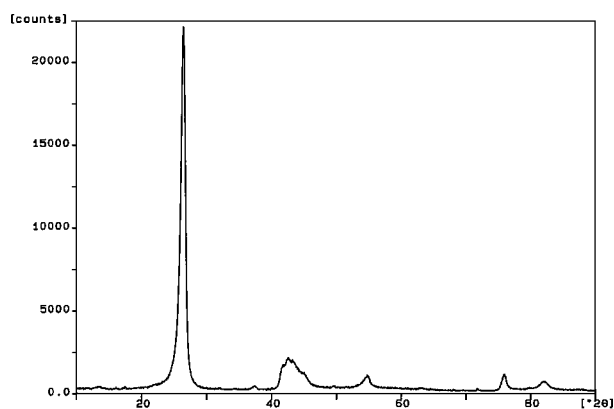

Figure 9 XRD powder pattern of the dried product after washing the material in Fig. 8 with 1 M HCl(aq.)

The iron and iron nitride phases were removed with dilute mineral acid leaving h-BN together with a trace amount of FeB_{49} which was presumed to be present in the original ferroboron starting alloy.

References
1. A. W. KIRBY and D. J. FRAY, *Trans. IMM.* **98** (1988) C33.
2. T. FUNAHASHI, T. KOITBASHI, R. UCHIMURA, T. KOSHIDA, A. YOSHIDA and T. OGASAWARA, Kawasaki Steel Technology Report N0. 28, June 1993.
3. R. KIESSLING and Y. H. LIU, *Journal of Metals* **19**(8) (1951) 639.
4. G. HÄGG, *Z. Physik. Chem.* **B7** (1930) 339.
5. D. F. SHRIVER, P. ATKINS and C. H. LANGFORD, "Inorganic Chemistry," 2nd ed. (Oxford, 1987).
6. HSC Chemistry Computer Software Data: Ver2.03, Outokumpu Research Oy, Poti, Finland.
7. V. RAGHAVAN, "Phase Diagrams of Ternary Iron Alloys" (ASM International, 1987) p. 219.
8. L. VEL, G. DEMAZEAU and J. ETOURNEAU, *Mats. Sci. Eng.* **B10** (1991) 149.